Kinetics of Interstitially Administered Monoclonal Antibodies for Purposes of Lymphoscintigraphy

Richard L. Wahl, Onelio Geatti,* Monica Liebert, Barry Wilson,† Paul Shreve, and Barbara A. Beers

University of Michigan Medical Center, Department of Internal Medicine, Division of Nuclear Medicine, Ann Arbor, Michigan

The clearance rates of radiolabeled murine monoclonal intact IgG, $F(ab')_2$ Fab and of an IgM following subcutaneous administration were evaluated in normal mice and rats using nuclear imaging and counting techniques. These studies suggest no significant difference in clearance rate exists between intact IgG and its $F(ab')_2$ fragment, and little difference between these moieties and intact IgM. Fab is cleared considerably faster than the others, however. While significant differences in clearance rates exist, the magnitude of the differences are not as large as those following intravenous injection particularly when ambulation by the animal is allowed. When ambulation is allowed, clearance rates of all classes and fragments are accelerated and quite similar. Injection into the subcutaneous tissues of the footpad results in consistently faster clearance than an injection into the subcutaneous tissues of the abdomen. Ambulation considerably increased the clearance of antibodies, presumably by increasing lymph flow. These studies imply that the choice of intact antibody versus fragments for kinetic reasons may be less critical (particularly if ambulation is allowed) by the subcutaneous as compared with the intravenous delivery route. This kinetic information should be useful in designing imaging protocols with radiolabeled antibodies administered subcutaneously for purposes of imaging disease processes involving the lymphatics.

J Nucl Med 28:1736–1744, 1987

The availability of monoclonal antibodies with high in vitro specificity for antigens has increased interest in their potential use as carriers of radioactivity to diagnose and treat tumors and other conditions (*1–4*). While monoclonal antibodies' in vitro specificity is often impressive, results in vivo have frequently been less striking following intravenous radioantibody administration, with only relatively low target/nontarget ratios being achieved in most cases (*5,6*). This problem has been in part addressed by the use of antibody fragments, in particular $F(ab')_2$ fragments, that have increased tumor/nontumor ratios, while their rapid clearance has resulted in earlier imaging times (*7–9*) than intact antibody.

Although improvements in tumor/nontumor ratios with antibody fragments are encouraging, a more dramatic improvement in tumor/nontumor ratios was described by Weinstein et al., who increased specific tumor-binding of monoclonal antibodies by administering the antibodies subcutaneously so that preferential uptake of the antibody molecules would be directed to lymph nodes draining the injection site (*10*). If these nodes were invaded by tumor cells, then the antibody directed against the tumor would specifically accumulate. This accumulation of tumor-specific antibody in nodal metastases of guinea pig hepatocarcinomas was considerably more than accretion of an equal amount of that antibody administered intravenously (*10*). We have recently shown this approach to be successful in detecting small nodal metastases of human xenografts of choriocarcinoma (*11*). Weinstein and others suggested that this high level of antibody uptake into tumor-containing lymph nodes was due to presence of

Received Feb. 11, 1986; revision accepted Mar. 12, 1987.

For reprints contact: Richard L. Wahl, MD, Division of Nuclear Medicine, University of Michigan Medical Center, 1500 East Medical Center Dr., Ann Arbor, MI 48109-0028.

* Present address: Intituto di Medicina Nucleare, Ospedale Civile, 33100-Udine, Italy.

† Hybritech Incorporated, Dept. of Cell Biology, 11095 Torreyana Rd., San Diego, CA 92121.

an intact basement membrane about blood vessels, but the lack of one about lymphatics, allowing for preferential uptake to the lymphatics (*10,12–14*).

While considerable differences in clearance from the body are seen among intact antibody and antibody fragments following intravenous administration (*7–9*), the influence of fragmentation and of antibody class has not been evaluated in assessing clearance of radiolabeled antibody from a subcutaneous injection site and thus the impact of these factors on potential imaging behavior. Similarly, the influence of the injection site location (central or peripheral) motion, or label have not been evaluated. Knowledge of antibody egress rates is critical to rationally selecting monoclonal antibodies for imaging following interstitial administration. In this study, we evaluate the kinetics of antibody clearance following subcutaneous administration, with the objective of determining if egress rates following local administration are affected significantly by class, fragmentation, location of injection (central or peripheral), motion or label, with an aim to selecting the antibody or fragment best suited to delivery by this route.

METHODS

Monoclonal Antibodies

The IgG 2ak murine monoclonal antibody 225.28S is reactive with the high molecular weight antigen of melanoma (*15*). It was grown in pristane-primed* BALB/c mice as ascites, and purified by staphylococcal protein A chromatography (*16*). Its $F(ab')_2$ fragment was prepared by 2% pepsin digestion in pH 4.2 acetate buffer with purification by dialysis versus Ph8 PBS and then on a staphylococcal protein A column (*7, 17*). The 225.28S Fab fragment was prepared by 2% papain digestion and purification of the Fab from the F-C on a staphylococcal protein A column (*7,18*). Additional purification by TSK3000 sizing high performance liquid chromatography (HPLC) was also conducted. FT166 is an IgM of murine origin, which was purified on DEAE chromatography from mouse ascites (Liebert M: unpublished data). None of these murine antibodies are known to cross-react with normal murine tissues. The molecular weight and purity of these reagents was verified on 7.5% SDS polyacrylamide gels with and without 2ME (*19*). In addition, the high molecular weight of the unreduced IgM was verified by TSK3000 sizing HPLC.

Radiolabeling

All iodine labelings were conducted using iodine-131 (^{131}I) or iodine-125 (^{125}I)†, by the iodobead method‡ (*20*). In general, labelings were conducted by reacting 1 mCi with 100 μg of antibody protein to yield a specific activity of ~6–8 μCi/ μg. Free iodine was removed from the mixture after labeling by Biogel P-60 sizing chromatography§. Iodine-131 was used for imaging. In nonimaging studies (with Fab), ^{125}I was used. The intact 225.28S was also labeled with ^{111}In† using diethylenetriaminepentaacetic acid (DTPA) chelation. Ten milligrams per milliliter 225.28S were prepared in a pH 8.1 sodium bicarbonate buffer. Cyclic DTPA anlydride¶ was dissolved in dimethyl foramide to a concentration of 3.0 mg/ml. For 2 hr 2.5 mg of 225.28S were reacted with a 5/1 DTPA/antibody ratio. Dialysis was then performed in pH 7 phosphate buffered saline. Three hundred microcuries of $InCl_3$† was then added and reacted overnight at 4°C. The protein bound ^{111}In was separated from free ^{111}In and DTPA by Biogel P-60 sizing chromatography**. A specific activity of ~0.12 μCi/μg was achieved (*21*).

Injection and Imaging

Adult female BALB/c mice were used for all imaging experiments. Mice were first sedated with 1.2 mg of pentobarbital i.p. After sedation and immobilization on an animal board, subcutaneous injections of ~10–15 μCi of antibody (30–50 μl) were made into groups of four mice, either into the hind foot pad or into the subcutaneous tissue of the mid-abdominal wall. Immediately after injection, the injection site was cleaned lightly with an alcohol wipe, and then gamma camera imaging was begun.

The initial imaging period was 6 hr. During this time period, animals remained sedated and immobilized, with occasional boosts of pentobarbital i.p. In additional experiments using the Fab iodinated fragments or the ^{111}In intact antibody, subgroups of animals were allowed to ambulate after the first 15-min image was obtained and then were reimaged (for 15 min) or recounted at 6 hr. In all cases imaging was conducted with a large field-of-view gamma camera equipped with a high-energy; parallel hole collimator. The 364-keV photopeak of ^{131}I was imaged with a 20% energy window. All images were recorded on film, as well as stored in a dedicated nuclear medicine computer (MDS A^2) using 15-min frames and a 128 × 128 pixel array, word mode, and 1.14 × magnification. The collimator to animal distance was fixed and identical for all acquisitions.

After 6 hr, imaging was terminated, and the mice were allowed to regain consciousness and ambulated. Subsequent imaging, using identical positioning and imaging parameters was undertaken at intervals from 18–60 hr following initial injection. Animals were re-sedated for these images. These acquisitions were also for 15-min frames, but only two such frames were acquired at these later time points. Identical acquisition parameters were used for these images. If activity at the injection site had faded markedly the injection site would be "marked" using a cobalt-57 marker, on a separate image, to aid in subsequent images analysis.

Image Analysis

Rectangular regions of interest (ROIs) over the injection site were manually drawn using the computer, as determined on the 0–15-min images and the counts over time in the ROI were computer-determined. These identically-sized regions were also drawn over the injection site on subsequent images' and images' counts analyzed. Background counts at each time point were also determined over time by selection of an identically-sized region of interest separate from the animals, and this value was used to correct the values for the regions of interest. Time-activity curves of radioactivity clearance are then plotted, after correction for ^{131}I or ^{111}In T ½.

Nonimaging Studies

To further evaluate the effect of ambulation on Fab of 225.28S, eight BALB/c mice were injected subcutaneously into the hind footpad with ~20 μCi of [^{125}I]Fab and then

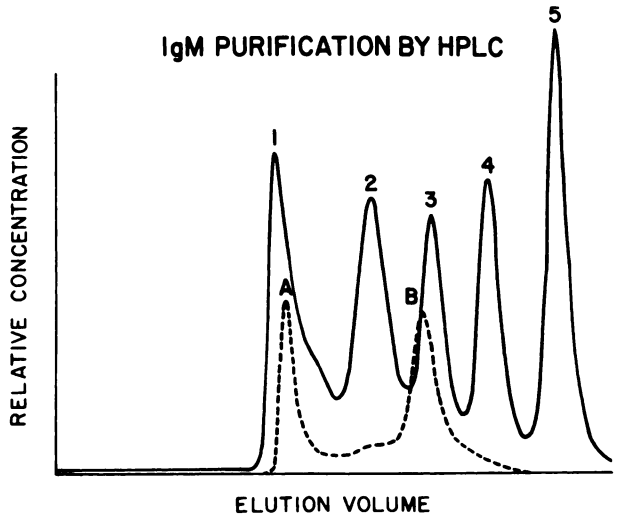

FIGURE 1
Shows the sizing (TSK3000) HPLC profile of IgM containing ascites, with the high molecular weight FT166 IgM peak (A) and albumin (B) indicated. Superimposed standards (1, 2, 3, 4, 5) indicate: thyroglobulin (700 kD); IgG (150 kD); ovalbumin (45 kD); myoglobin (17 kD); and cyanocobalamin (1.35 kD).

one group was allowed to ambulate while the other was kept sedated. After 6 hr, the feet were surgically removed after killing the animal and counted in a dose calibrator.

The relative uptake of [^{125}I] IgM FT166 to lymph nodes was also studied in normal female Sprague-Dawley rats. Sixteen such rats were injected into the right hind footpads with 4–5 μCi and four were killed at 0.33, 1, 2, and 4 hr postinjection. At these times blood, ipsilateral and contralateral popliteal node, and liver activities and weights were determined. This nonimaging studies allow for the time course of nodal and blood uptake to be evaluated.

Statistical Analysis

The two-way analysis of variance method, the Student's t-tests and the Bonferroni method of multiple comparison was used in data analysis.

RESULTS

Integrity of Antibodies and Fragments

SDS polyacylamide gels using nonreducing conditions documented excellent purity of the antibody and fragment preparations. Sizing HPLC of FT166 ascites showed that the IgM, FT166, eluted at a high molecular weight compatible with IgM (Fig. 1).

Clearance Rates for Intact IgG Versus Fragments Versus IgM

Each antibody and fragment was evaluated for clearance following subcutaneous injection. Images from the early portion of a representative experiment are shown in Figure 2. This demonstrates that following the injection of intact IgG into the footpad of four BALB/c mice that there is a gradual decrease, in the first 6 hr, of activity from the foot with an increase in the whole-body activity (Fig. 2A and 2B). By 18 hr, postinjection activity is still present (Fig. 2C) in the footpad with more in the body. Rectangular ROIs were drawn over the injection sites and used to generate the time-activity curves for clearance (Fig. 2D).

As is shown in Figure 3, the clearance rates of the varying antibodies and fragments following a subcutaneous injection into the skin of the right abdomen are parallel to each other. Statistical analysis at the 6-hr time point (no motion from 0–6 hr by the animals) demonstrates that F(ab')$_2$, IgM and intact IgG antibody have similar rates of clearance, while Fab clearance is significantly faster ($p < 0.0002$) than these three (Table 1). Calculated $T_{½}$'s of clearance from the injection site in the first 6 hr without motion are indicated in Table 2.

Figure 4 illustrates the clearance from the injection site of the varying antibodies and fragments following a subcutaneous injection into the footpad. In the first 6 hr postinjection, while the animals are immobilized, there is again no statistically significant difference in clearance rates between intact IgG and F(ab')$_2$, while IgM exits significantly more rapidly ($p = 0.0118$) and Fab still faster ($p < 0.0001$) (Table 1). Extrapolated $T_{½}$'s for clearance from these locations without motion are indicated in Table 2.

Influence of Location of Injection

Figures 5A, B, C, and D show the comparative egress rates between foot pad and subcutaneous tissues of the ventral abdomen injection sites of antibodies. In general, the ventral abdominal subcutaneous route of injection has slower egress than the footpad injection site. This difference in clearance rates between injection locations is statistically significant ($p = 0.0002$) as is shown in Table 2.

Effects of Motion

The $T_{½}$ of antibody egress was assessed before and after ambulation was allowed. As indicated in the methods section, this ambulation was studied in two ways. In the initial imaging experiments, ambulation was allowed to begin 6 hr after antibody or fragment injection. As is noted in the curves in Figures 3–4 and especially 5 (with a semilog plot; as well as in Table 2), this ambulation results in considerately more rapid disappearance of antibody from the injection site than was present when the animal was sedated.

Effects of immediate ambulation were also studied in animals injected with iodinated Fab and ^{111}In intact antibody. In imaging experiments two animals in addition to the two groups of four studied above were injected subcutaneously into the hind footpad with the ^{131}I Fab fragment and then, after initial images were obtained for 15 min, were allowed to ambulate. They were then reimaged at 6 hr after injection, at the same

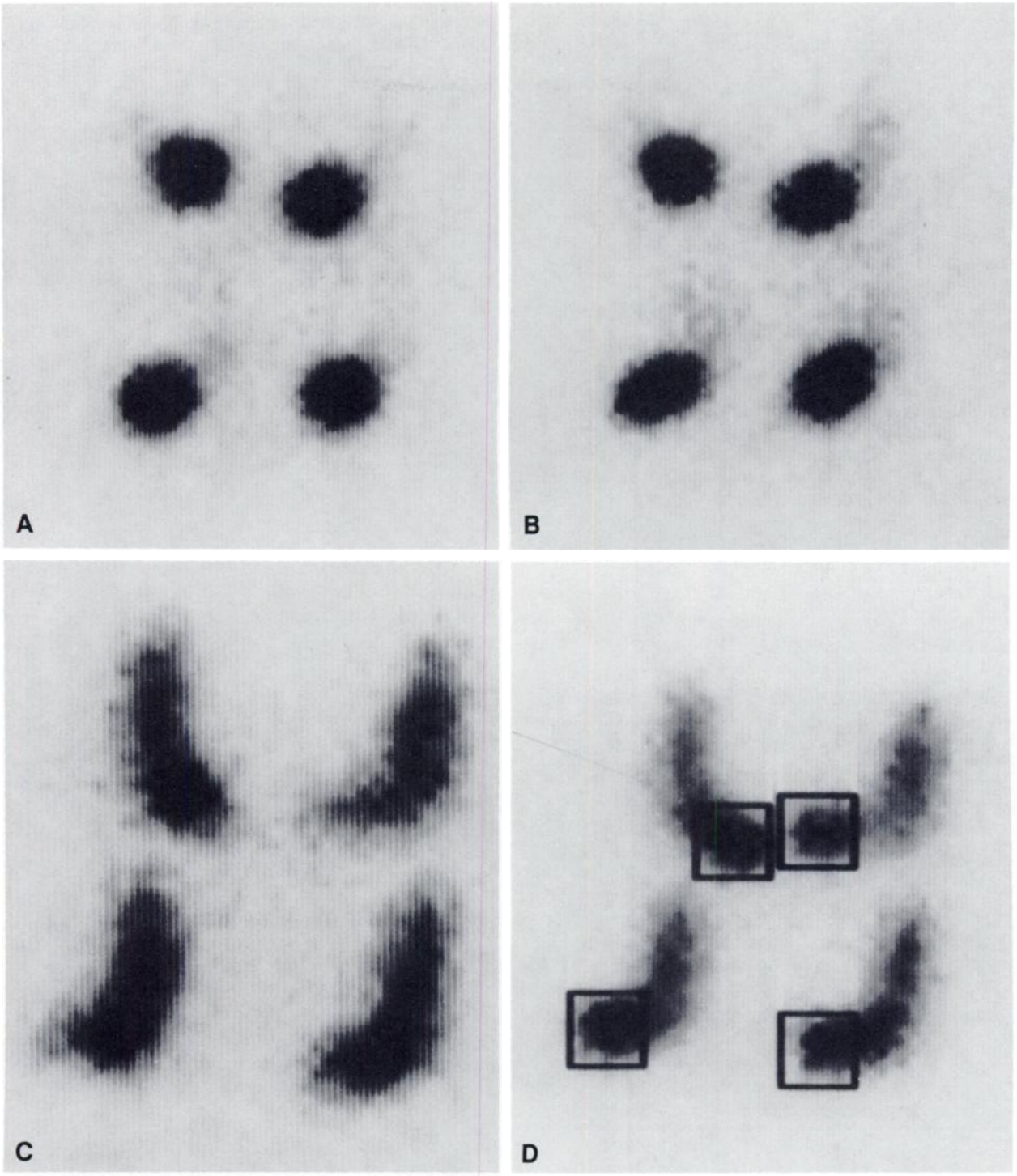

FIGURE 2
0 hr (A), 6 hr (B), and 18 hr (C) images of four mice injected with [^{131}I] intact antibody into the hind footpads. Note gradual loss of activity from the feet, and resulting increase in whole-body activity. (D) Representative illustration of images generated by gamma imaging of four mice ~1 day following injection of radiolabeled antibody into footpads. Each square region of interest is used to generate a time-activity curve reflecting antibody egress (see text).

time that four other animals who had been injected in the footpad and which had been immobilized, were having their continuous imaging terminated. Thus, two animals ambulated freely following injection, and four were immobilized throughout the first 6 hr of imaging. The clearance was significantly faster in the ambulatory animals ($p < 0.0001$) (Fig. 5C and Table 2). This result was confirmed in an ^{125}I Fab study in which eight

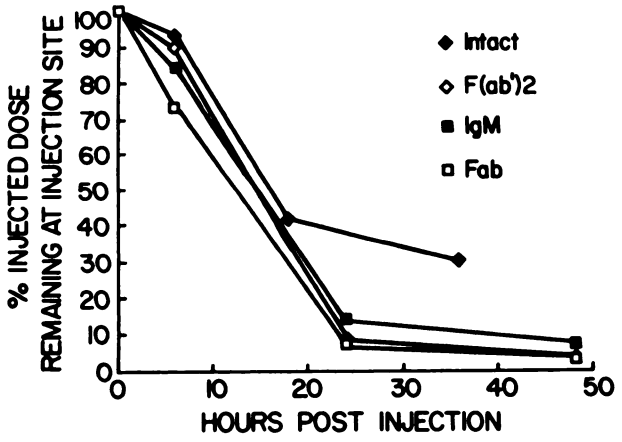

FIGURE 3
Clearance of antibodies and fragments following subcutaneous injection into ventral abdominal wall. No motion (ambulation) was allowed from 0–6 hr. Ambulation was then allowed for the duration of the study. The percent of residual activity values are corrected for ^{131}I decay. Note faster clearance with motion, plotted linearly.

TABLE 2
Extrapolated $T_{½}$ of Clearance from Injection Site With and Without Motion (Ambulation) in hr (from Table 2)

	Abdominal wall		Footpad	
	No motion	Motion*	No motion	Motion*
Intact IgG	44	13	22	5.5
$F(ab')_2$	32	5	32	4
IgM	18	4	12	4
Fab	14	7	6.4	3.72†

Data for "no motion" (no ambulation) linearly extrapolated based on exponential clearance rate from T = 0–6 hr without animal ambulation. Clearance rates, when ambulation was allowed were considered faster and are calculated based on measured clearance rates from 6–24 hr plotted exponentially.

* Ambulation increases the rate of antibody egress at $p < 0.0001$.

† Except Fab injected into the foot where due to fast clearance without ambulation the effect of ambulation was studied from 0–6 hr, see text.

animals were injected into the footpad with ~20 μCi of Fab each. Four were allowed to ambulate, while four did not. Those that ambulated had just 6.02 ± 1.91% (s.d.) of the injected dose remaining at 6 hr (by dose calibration), while the sedated nonambulatory animals had 44.9 ± 6.46% (s.d.) remaining (significantly different at $p < 0.0005$), (Fig. 6).

The clearance rate of ^{111}In 225.28S intact was evalu- foot pad activity at 6 hr without ambulation was 82.75 ± 1.23% (s.d.). This was significantly more ($p < 0.0005$) than the group allowed to ambulate which had 31.8 ± 3.06% (s.d.) remaining (Fig. 7). Also of note is that the clearance of In and iodine labeled intact monoclonal antibody are quite comparable at 6 hr (82.75% remains for ^{111}In and 85.1% remains for ^{131}I).

Uptake in Other Tissues and Draining Nodes

The uptake of the IgM, FT166 was evaluated in normal rats following foot pad injection. The results, shown in Table 3, indicate that high levels of IgM are achieved in the popliteal node ipsilateral to the injection at early time points. Node/blood ratios are consistently >100, indicating high level uptake to the regional draining nodes.

TABLE 1
Percent of Activity Remaining at the Injection Site Following Subcutaneous Injection Without Ambulation by Animals

	Decay-corrected activity remaining 6 hr postsubcutaneous injection (± s.d.)			
	Abdominal wall		Foot*	
Intact IgG	93.3 ± 1.85		85.1 ± 6.93	
$F(ab')_2$	89.6 ± 3.37	N.S.	86.4 ± 1.85	N.S.
IgM	84.2 ± 4.21		73.0 ± 9.67†	
Fab	73.1 ± 4.85‡		52.9 ± 9.12§	

N = three or four animals/group; all antibodies labeled with ^{131}I.

* Clearance from the foot is significantly ($p = 0.0002$) faster than from the abdominal wall.

† Different from footpad injection of intact, IgG and $F(ab')_2$ at $p < 0.02$.

‡ Different from abdominal wall injection of intact, IgM and $F(ab')_2$ at $p = 0.0002$.

§ Different from footpad injection of intact IgG, $F(ab')_2$ and IgM at $p < 0.003$.

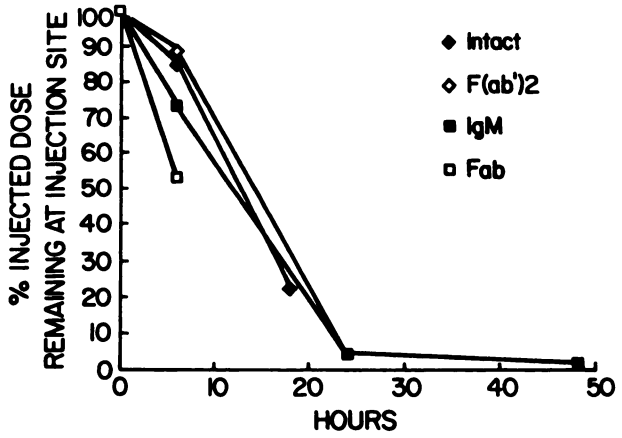

FIGURE 4
Clearance of antibodies and fragments following subcutaneous injection into the footpad. No animal motion was allowed from 0–6 hr. Ambulation was then allowed for the duration of the study. The percent of residual activity values at the injection site are corrected for ^{131}I decay. Note faster clearance with ambulation, plotted linearly.

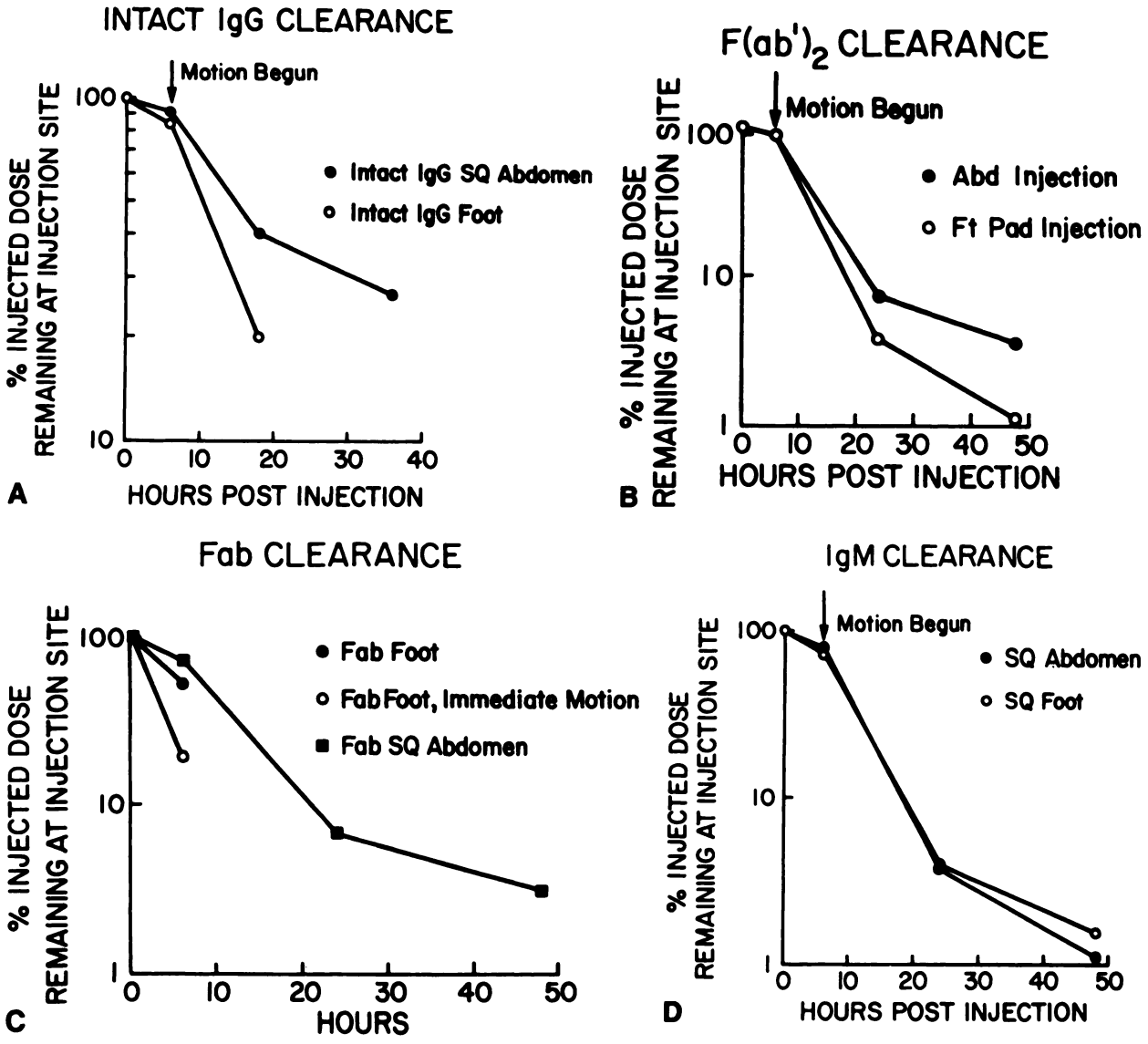

FIGURE 5

A–D: Clearance of iodinated intact IgG (5a), $F(ab')_2$ (5b), Fab (5c) and IgM (5d), from the footpad or abdominal wall plotted on a semilog scale. Note that footpad clearance is in general more rapid than clearance from the abdominal wall injection site. Also note that ambulation increases clearance rates considerably ($p < 0.0001$). In 5C note that immediate ambulation was allowed in one group of animals injected into the foot, resulting in a very rapid egress rate.

DISCUSSION

Monoclonal antibodies reactive with tumor-associated antigens hold considerable promise in the detection of human tumors. The realization of this promise has been slow because of the relatively low tumor/nontumor ratios achieved by intact antibodies given intravenously, and the temporal delays in achieving optimal target levels (*6,7*). Antibody fragments have alleviated this problem to some extent; however, the subcutaneous route of antibody administration (so that a considerable portion of the dose migrates intralymphatically) appears to have more of an ability to detect smaller foci of tumor than the intravenous route (*7,10*). In our animal experiments using human tumors (*11*) and in the work of Weinstein (*10*), optimal tumor imaging following the subcutaneous route occurred well before the expected optimal time for visualization following i.v. delivery. In experiments we and others have conducted in the past several years, antibody fragments appear capable of earlier tumor visualization than intact antibody (*7,9*). The kinetics of these fragments following subcutaneous administration have not been studied, however.

In this investigation, we have demonstrated that murine IgG2a and its $F(ab')_2$ administered subcutaneously are removed at relatively similar rates from the injection site. The Fab fragment exited the injection site significantly faster than the IgG or $F(ab')_2$ fragments. The

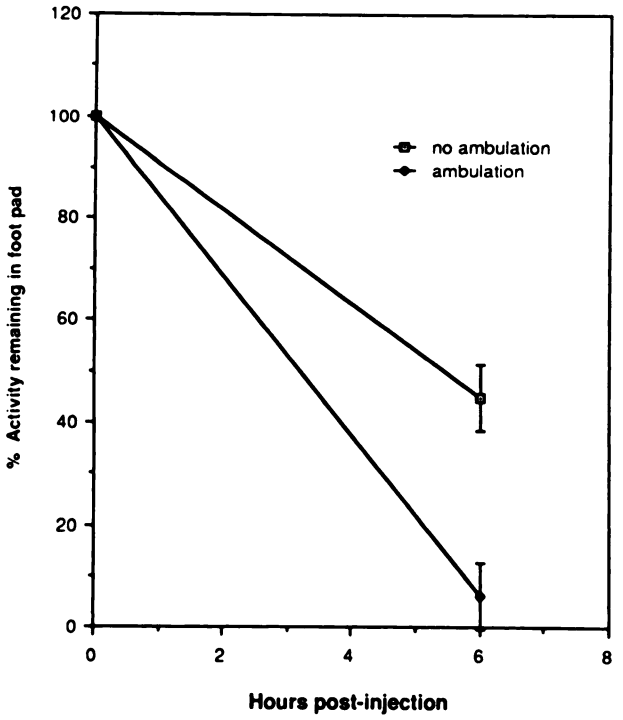

FIGURE 6
Clearance of [^{125}I] Fab of 225 measured by dose calibration following footpad injection with and without ambulation. Note the significant acceleration in clearance due to ambulation ($p < 0.0005$).

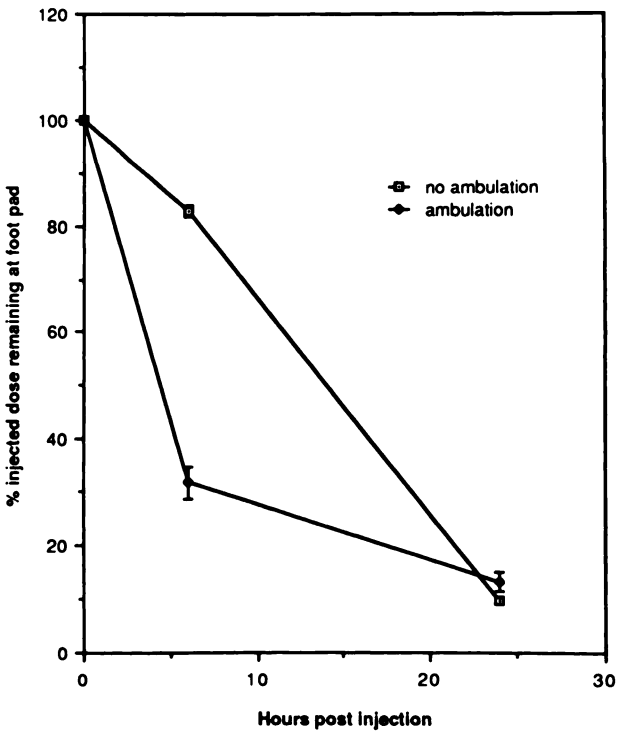

FIGURE 7
Linear plots showing gamma camera measured clearance (mean ± s.d.) of [^{111}In] intact 225.28S from footpad. Ambulation animals (N = 4) were allowed to move freely from 15 min postinjection until 24 hr postinjection. Nonambulatory animals (N = 4) were kept motionless from 0 to 6 hr postinjection, and then ambulated freely until 24 hr. Note the significant differences at 6 hr between groups ($p < 0.0005$).

IgM's clearance was intermediate. An important route of egress following such injections is through the lymphatic system (*12–14*). This apparently is because of the presence of an intact basement membrane about blood vessels in the subcutaneous regions, while at the same time there is a lack of such an intact membrane about lymphatics that allows for preferential absorption of large molecules (such as antibodies) into lymph channels, to lymph nodes and eventually to the blood stream (*12–14*). Naturally, some absorption by the blood directly will occur. The partitioning of uptakes to lymph and blood have been modeled (*12*). The current study does not attempt to separate these two components, but the blood and node data we present for the IgM antibody in rats shows that high levels of monoclonal antibody do reach the lymph nodes. In other studies, we have shown that IgG antibody achieves high uptake to draining nodes, but this apparently is less than for IgM (*22*).

Not surprisingly, since lymph flow is increased when motion is present (*23*) clearance of radiolabeled antibodies is accelerated when motion occurs, particularly motion of an extremity. This is of potential practical importance in patient studies, as it could markedly decrease radiation absorbed dose at the injection site and accelerate delivery of antibody to regional draining lymph nodes.

Location of injection in mice made a significant

TABLE 3
Uptake to Blood and Nodes of [^{125}I]FT166 Following Subcutaneous Injection

	20 min	1 hr	2 hr	4 hr
Ipsilateral popliteal node	102.06 ± 40.3	64.20 ± 3.76	62.93 ± 17.63	32.35 ± 6.44
Contralateral popliteal node	0.0128 ± 0.076	0.051 ± 0.008	0.243 ± 0.158	0.056 ± 0.008
Blood	0.087 ± 0.003	0.129 ± 0.0096	0.134 ± 0.015	0.144 ± 0.015
Liver	0.0368 ± 0.0029	0.0607 ± 0.0055	0.050 ± 0.0057	0.045 ± 0.004

Mean % kg injected dose/g in groups of four female Sprague Dawley rats ± s.e.m., at varying times post-footpad injection of 4–5 μCi of [^{125}I]FT166 (IgM). Note high levels of antibody in popliteal nodes ipsilateral to injection site.

difference as well, with the subcutaneous injection site in the abdominal wall having significantly slower clearance than the foot. This was particularly apparent with ambulation, implying an ability of lymph flow to increase more in the foot with ambulation than it does in the ventral abdominal wall. There is, however, the potential of our scintigraphic method of exam to underestimate clearance rates from the mid-abdominal wall due to residual blood-pool activity. This was corrected for, in part, by selecting a background ROI for correction.

These studies also demonstrate, particularly with the Fab and IgM, that some deiodination is ongoing, as on later images some uptake of ^{131}I is noted in the thyroid gland (which was deliberately left unblocked). Such deiodination will no doubt occur in man as well as may increase the apparent clearance rate. It is possible that the more rapid clearance of the Fab may be partially related to its deiodinating more rapidly than intact antibody in certain instances (*7*). The clearance rate of indium-labeled intact antibody in our study was similar to that of iodinated antibody, suggesting deiodination is not occurring at high levels (*23*).

Thus, while differences do exist in the clearance rates of antibodies and their fragments following subcutaneous injection, the differences are not as marked as those seen following i.v. injection. If motion occurs, increasing lymph flow, all agents studied clear quite rapidly, and at very similar rates. These clearance data should aid in planning lymphoscintigraphic studies with radiolabeled antibodies.

NOTES

* Aldrich Chemical Company, Milwaukee, WI.
† Du Pont Company, No. Billerica, MA.
‡ Pierce Chemical, Rockford, IL.
§ Biorad Incorporated.
¶ Sigma Chemical Corporation, St. Louis, MO.
** BioRad Laboratories.

ACKNOWLEDGMENTS

The authors thank Mrs. Michele Bell for excellent secretarial assistance in the preparation of the manuscript and Mr. Carl Dmuchowski for statistical assistance. Mr. Jon Johnson, Ms. Linda Laino and Mrs. Gayle Jackson provided valuable technical assistance.

This work was supported in part by DOE #DE-AC02-76EV02031; NCI #7R01 CA33802-01; NCI #1R01 CA-40497-01; and NCI #1R01 CA41531-01.

REFERENCES

1. Ballou B, Levine G, Hakala TR, et al. Tumor location detected with radioactively labeled monoclonal antibody and external scintigraphy. *Science* 1979; 206:844–846.
2. Mach JP, Buchegger F, Forni M, et al. Use of radiolabelled monoclonal anti-CEA antibodies for the detection of human carcinoma by external photoscanning and tomoscintigraphy. *Immunol Today* 1981; 2:239–249.
3. Larson SM, Carrasquillo JA, Krohn KA. Radiotherapy with "anti-p97" iodinated monoclonal antibodies in melanoma. In: Proceedings for the Third World Congress on Nuclear Medicine and Biology. Vol. 4. Paris, New York: Pergamon Press, 1982:3666–3669.
4. Wahl RL, Parker CW. Monoclonal antibody radioimmunodection of transplant rejection. *Transplantation* 1985; 40:451–454.
5. Wahl RL, Philpott G, Parker CW. Monoclonal antibody radioimmunodetection of human-derived colon cancer. *Invest Radiol* 1983; 18:58–62.
6. Larson SM, Carrasquillo JA, Krohn KA, et al. Diagnostic imaging of malignant melanoma with radiolabeled antitumor antibodies. *JAMA* 1983; 249:811–812.
7. Wahl RL, Parker CW, Philpott GW. Improved radioimaging and tumor localization with monoclonal $F(ab')_2$. *J Nucl Med* 1983; 24:316–325.
8. Colcher D, Zalutsky M, Kaplan W, et al. Radiolocalization of human mammary tumors in athymic mice by a monoclonal antibody. *Cancer Res* 1983; 43:736–742.
9. Buchegger F, Haskell CM, Schreyer M, et al. Radiolabeled fragments of monoclonal antibodies against carcinoembryonic antigen for localization of human colon carcinoma grafted into nude mice. *J Exp Med* 1983; 158:413–427.
10. Weinstein JN, Steller MA, Keenan AM, et al. Monoclonal antibodies in the lymphatics: selective delivery to lymph node metastases of a solid tumor. *Science* 1983; 222:423–426.
11. Wahl RL, Jackson G, Laino L, et al. Improved radioimmunolocalization of human-derived tumors by intralymphatic delivery of monoclonal antibodies. *Radiology* 1984; 153:316.
12. Bergqvist L, Strand S-E, Persson BRR. Particle sizing and biokinetics of interstitial lymphoscintigraphic agents. *Semin Nucl Med* 1983; XIII:9–19.
13. Leak LV. Studies on the permeability of lymphatic capillaries. *J Cell Biology* 1971; 50:300–323.
14. Weinstein JN, Steller MA, Covell DG, et al. Monoclonal antitumor antibodies in the lymphatics. *Cancer Treat Rep* 1984; 68:257–264.
15. Wilson BS, et al. Distribution and molecular characterization of a cell surface and cytoplasmic antigen detectable in human melanoma cells with monoclonal antibodies. *Int J Cancer* 1981; 28:293–300.
16. Ey P, Prowse S, Jenkins C. Isolation of pure IgG_1, IgG_{2a}, and IgG_{2b} from mouse serum using protein A-Sepharose. *Immunochem* 1978; 15:429–436.
17. Burchiel SW, Khaw BA, Rhodes BA, et al. Immunopharmacokinetics of radiolabelled antibodies and their fragments. In: Burchiel SW, Rhodes BA, eds. Tumor imaging. New York: Masson Publishing, 1982:125–140.
18. Porter RR. The hydrolysis of rabbit gamma globulin and antibodies with crystalling papain. *Biochem J* 1959; 73:119.
19. Laemmli VK. Cleavage of structural proteins during assembly of the head of bacteriophage T4. *Nature* 1970; 222:680–685.

20. Markwell MAK. A new solid-state reagent to iodinate proteins. I. Conditions for the efficient labeling of antiserum. *Anal Biochem* 1982; 125:427–432.
21. Hnatowich DJ, Childs RL, Lanteigne D, et al. The preparation of DTPA-coupled antibodies radiolabeled with metallic radionuclides: an improved method. *J Immunol Meth* 1983; 65:147–157.
22. Wahl RL, Fisher S, Petry NA. Antibodies, albumin and antimony: comparison of three lymphoscintigraphic agents. *Radiology* 1986; 161:322.
23. Baez S. Flow properties of lymph. A microcirculatory study. In: Copley AL, Stainsby G, eds. Flow properties of blood and other biological systems. New York: Pergamon Press, 1960:398–411.
24. Halpern SE, Hagan PL, Garver PR, et al. Stability, characterization, and kinetics of ^{111}In-labeled monoclonal antitumor antibodies in normal animals and nude mouse-human tumor models. *Cancer Res* 1983; 43:5347–5355.